Synthesis, Crystal Structures, Dielectric, and Magnetic Properties of Manganese-Sulfonyldibenzoate

Balendra,*[a, b] Bharti Singh,[a] Azeem Banday,[c] Shailabh Tewari,[a] Vineet Kumar,[a] Sevi Murugavel,[c], Pattayil Joy[d] and Arunachalam Ramanan*[a]

[a]*Department of Chemistry, Indian Institute of Technology Delhi, Hauz Khas, New Delhi-110016, India*

[b] Department of Chemistry, Sri Venkateswara College (University of Delhi) Dhaula Kuan Delhi-110021, India

[c]*Department of Physics and Astrophysics, University of Delhi, Delhi-110007, India*

[d]*CSIR-National Chemical Laboratory, Pune, 411008, India*

E-mail: *aramanan@chemistry.iitd.ac.in*. Tel: +91-11-26591507. Fax: +91-11-26581102.

E-mail: balendra.iitr@gmail.com.

Chemistry of Mn-SBA and auxiliary ligand-based system.

Mn(II) is known to form discrete higher nuclear clusters, which act as SBUs in the construction of multidimensional networks. Present work details the formation of new manganese sulfonyl dibenzoate based CPs. The available literature suggested that an additional auxiliary ligand (preferably N-donor ligand) helps to provide phase suitable for single-crystal X-ray crystallography with diverse structural features (Table S1).To understand the Mn-*SBA* system with auxiliary ligands, we carried out a literature survey based on *SBA* ligand using CSD database[1] analysis. It showed 323 hits out of which 240 are with transition metals. The lanthanides have 35 hits whereas alkaline-earth metals showed only 30 hits (Fig S1a). By further narrowing the CSD search, we found that only 30 structures are reported with Mn (II), 4,4'-sulfonyldibenzoic acid and different N-donor ligands; interestingly the SBUs in these solids varied from dimer to pentamer (Fig S1b).
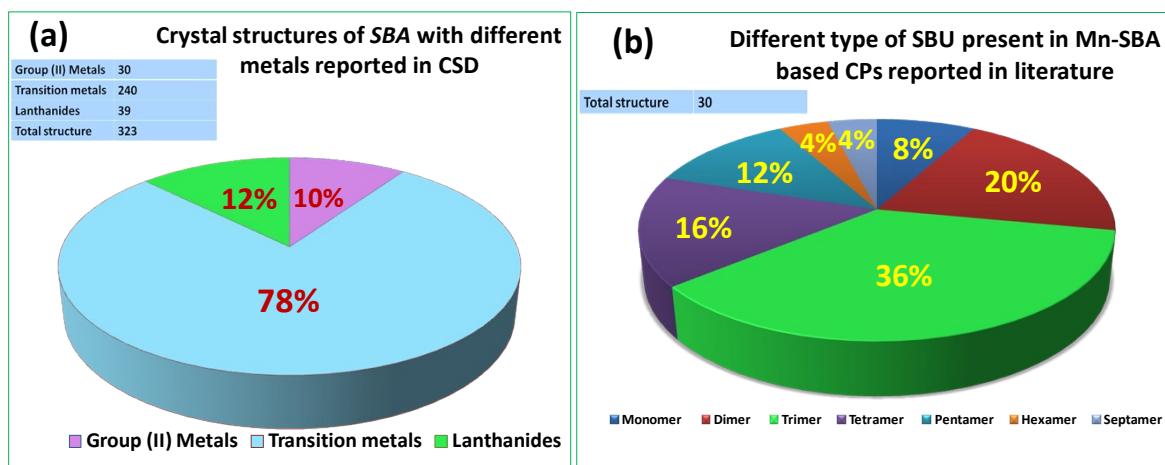
Fig. S1 (a) Number of solids reported in the database containing *SBA* and different metal ions. (b) Percentage of different SBU present in the Mn-*SBA* system reported in the literature.

Table. S1 Structural diversity of manganese-*SBA*-auxiliary ligand system reported in the literature. The table also includes the six solids prepared in this study for comparison.

| Solids	Mn Centre	Geometry of manganese	Connectivity within the solids	Illustration of the cluster chain in the solids	Magnetic behaviour
[Mn(*SBA*)(2,2-bpy)][2]	Mn(1)	Distorted Octahedron	Two distorted octahedra are bridged by the *SBA*$^{2-}$ ligand to form the Mn-O-Mn 1D chain	[Mn$_2$O$_8$N$_4$] Dimer	Not reported
	Mn(2)	Distorted Octahedron			
[Mn(*SBA*)(*phen*)(H$_2$O)] .2DMA **5**	Mn(1)	Distorted Octahedron	Two different polyhedra are connected by the *SBA*$^{2-}$ ligand to form the 2D network.	[Mn$_2$O$_7$N$_4$] dinuclear	Antiferromagnetic χ_MT per Mn$_2$ unit at 300K = 9.37 emu K mol^{-1} Oe^{-1} θ = -9.59 K
	Mn(2)	Distorted square-pyramid			
[Mn$_4$(OH$_2$)$_2$(*SBA*)$_4$(*bpp*)$_4$][3]	Mn(1)	Distorted Octahedron	Four Mn atoms are bridged by two μ_2-OH$_2$ molecules and six carboxylate groups to form a tetranuclear manganese unit as a secondary building unit. Each tetrametallic unit is further interconnected by eight *SBA*$^{2-}$ ligands and six *bpp* ligands to generate 2D network	[Mn$_4$O$_{16}$N$_6$] tetranuclear	Antiferromagnetic χ_MT per Mn$_4$ unit at 300K = 16.366 cm^3 mol^{-1} K θ = -15.044K
	Mn(2)	Distorted Octahedron			
[Mn$_2$(*SBA*)$_2$(*btb*)$_{0.5}$(H$_2$O)][3]	Mn(1)	Distorted square-pyramid	The Mn1 and Mn2 centers are connected by four carboxylate groups of *SBA*$^{2-}$ ligands to form a paddle-wheel shaped dinuclear manganese unit. This dinuclear unit is further connected to another unit to form the 1D quadruple chains.	[Mn$_2$O$_9$N$_1$] dinuclear	Not reported
	Mn(2)	Distorted square-pyramid			
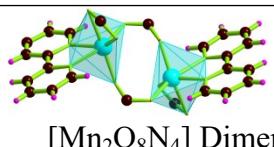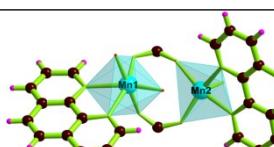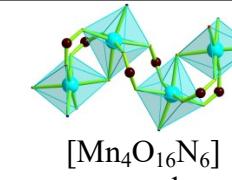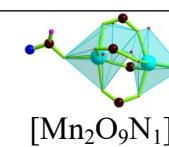
$[Mn_4(SBA)_4(bim)(H_2O)_4]\cdot 2H_2O$ [3]	Mn(1)	Distorted octahedron	Four Mn atoms are bridged by eight carboxylate groups to produce a tetranuclear manganese unit. Two neighboring tetranuclear manganese units are further linked by four SBA^{2-} ligands to generate 3D structure	$[Mn_4O_{18}N_2]$ tetranuclear	Antiferromagnetic $\chi_M T$ per Mn_4 unit at 300K = 16.834 cm³ mol⁻¹ K θ = -9.216K
	Mn(2)	Distorted square-pyramid			
$[Mn_5-(\mu_3-OH)_2(SBA)^4(2,2-bpy)_2(H_2O)_2]\cdot H_2O$ [4]	Mn(1) Mn(2) Mn(3)	All adopt distorted octahedron	The six coordinated Mn1centre is connected to four adjacent Mn centers in a corner- and/or edge sharing mode to form a $[Mn_5(\mu_3-OH)_2(\mu_3-O)_2]$. Each pentanuclear manganese cluster is further linked to six others through six triply bridging $SBA^{2-}$and four doubly bridging SBA^{2-}ligands to generate a 2D network	$[Mn_5(\mu_3-OH)_2(\mu_3-O)_2]$. pentanuclear	Antiferromagnetic $\chi_M T$ per Mn_5 unit at 300K = 21.027 cm³ mol⁻¹ K θ = -19.119K
$[Mn_5(SBA)_4(X)_2(DMA)_4]\cdot 4DMA$ X=2-*pic* in **1** X= *pyz* in **3** X= *mpyz* in **4**	Mn(1) Mn(2) Mn(3)	All adopt distorted octahedron	The pentameric cluster $\{Mn_5N_2O_{24}\}$ acting as SBU unit contains three corners shared octahedral polyhedrons as central atom Mn(1) occurred at inversion centered occupying at the special position the other part of the pentameric cluster generated automatically by symmetry. Each Mn_5 SBU units are connected to other four units by the SBA^{2-} ligands to form the 2D structure	$\{Mn_5N_2O_{24}\}$ pentanuclear	Antiferromagnetic $\chi_M T$ per Mn_5 unit at 300K =21.75 emu K mol⁻¹ Oe⁻¹ (**1**), 22.91 emu K mol⁻¹ Oe⁻¹(**3**), and 20.50 emu K mol⁻¹ Oe⁻¹ (**4**) θ =-21.01 K (**1**), -32.25 K (**3**), and -25.80 K (**4**)
$[Mn(SBA)(EtOH)]$ [5]	Mn(1)	Distorted octahedron	The inorganic motif displays 1D chain, formed by the corner-sharing MnO_6polyhedra. These chains are linked together by the SBA^{2-} ligands in two directions to generate the 2D network.	$[MnO_6]$ extended mononuclear	Not reported
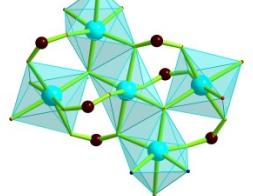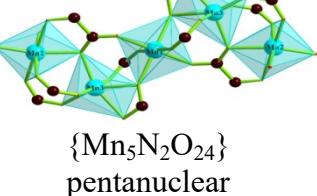
$[Mn(SBA)(H_2O)]^5$	Mn(1)	Distorted octahedron	The inorganic 1D chains, which are formed by the edge-sharing Mn_2O_{10} that are connected by SBA^{2-} ligand units. These chains are further linked together by the μ_5-links of SBA^{2-} ligands in two directions to generate the 2D structure	$[Mn_2O_{10}]$ dinuclear	Not reported
$[Mn(SBA)(phen)_2(H_2O)].3H_2O^6$	Mn(1)	Distorted octahedron	Complex 1 is an isolated-molecule, where carboxylic groups of SBA^{2-} ligand are deprotonated and provides an oxygen atom to bond to the Mn(II) center,	$[MnO_6]$ discrete monomer	Not reported
$[Mn_2(SBA)_2(H_2O)(py)_4]^6$	Mn(1) Mn(2)	Both adopt distorted octahedron	H_2O links the Mn(1) and Mn(2) to a binuclear metal unit, where SBA extend it 3D network	$[Mn_2O_8N_4]$ dinuclear	Antiferromagnetic $\chi_M T$ per Mn_2 unit at 300K = 8.60 cm^3 mol^{-1} K θ = -18.9K
$[Mn_3(SBA)_2(HSBA)_2(2,2\text{-}bipy)_2]^6$	Mn(1) Mn(2)	Both adopt distorted octahedron	SBA^{2-} ligands link the tri-nuclear SBUs into 1D chain with the other kind of SBA^{2-} ligands stretching out along the c direction. The two protonated carboxylic groups link to each other through two pairs of hydrogen bonding which extend the 1D chain to the 2Dstructure.	$[Mn_3O_{12}N_3]$ trinuclear	Antiferromagnetic $\chi_M T$ per Mn_3 unit at 300K = 12.78cm^3 mol^{-1} K θ = -2.14K
$[Mn_3(SBA)_2(pyz)_2(DMF)(H_2O)].DMF.H_2O$ **2**	Mn(1)	Distorted pentagonal bipyramid	The trimeric $\{Mn_3N_2O_{14}\}$SBU unit contains two edges shared polyhedron, as central atom Mn(1) occurred at inversion centered occupying at the special position which gives rise to a timer through symmetry translation. The	$[Mn_3N_2O_{14}]$ trinuclear	Antiferromagnetic $\chi_M T$ per Mn_3unit at 300K = 13.80 emu K mol^{-1} Oe^{-1}, θ = -7.07 K
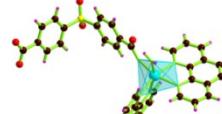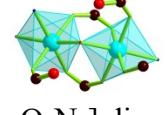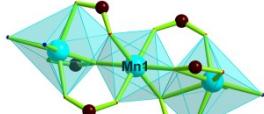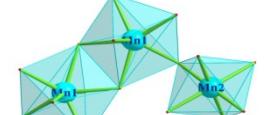
	Mn site	Geometry	Structure description	Cluster image	Magnetic properties
	Mn(2)	Distorted octahedron	continuous chain of trimeric units are bridged by the *SBA*$^{2-}$ ligand forming a 2D structure		
[Mn$_3$(*SBA*)$_3$(*phen*)$_2$].5DMF **6**	Mn(1) Mn(2) Mn(3)	All adopt distorted octahedron	The trimeric SBU {Mn$_3$N$_2$O$_{14}$} unit contains three corners shared polyhedron. The continuous chain of trimeric units is bridged by the *SBA*$^{2-}$ ligand forming a 2D structure.	[Mn$_3$N$_4$O$_{12}$] trinuclear	Antiferromagnetic χ_MT per Mn$_3$ unit at 300K = 12.13 emu K mol^{-1} Oe^{-1}, θ = -15.74 K
[Mn$_4$(*SBA*)$_4$(4-mepy)$_2$ (H$_2$O)$_4$].2H$_2$O[6]	Mn(1)	Distorted octahedron	Solid contains a tetra-nuclear Mn(II) cluster SBU unit which is extended by the *SBA*$^{2-}$ ligand to form the 1D network	[Mn$_4$O$_{20}$N$_2$] tetranuclear	Antiferromagnetic χ_MT per Mn$_4$ unit at 300K = 14.90 cm^3 mol^{-1} K θ = -8.6218K
	Mn(2)	Distorted square-pyramid			
[Mn$_4$(*SBA*)$_4$(bpp)$_4$(l-H$_2$O)$_2$]0.5H$_2$O[6]	Mn(1) Mn(2)	Distorted octahedron	Solid adopts a2D structure with tetra-nuclear Mn(II) cluster SBU unit extended by the *SBA*$^{2-}$ligand to form the 2D network	[Mn$_4$O$_{18}$N$_6$] tetranuclear	Antiferromagnetic χ_MT per Mn$_4$ unit at 300K = 12.49 cm^3 mol^{-1} K θ = -23.08K
[Mn$_5$(*SBA*)$_4$(*HSBA*)$_2$].4.5H$_2$O[7] and [Mn$_5$(NH$_4$)$_2$(*SBA*).2H$_2$O[7]	Mn(1) Mn(2)	Distorted octahedron	Distorted square pyramidal Mn is edge shared with octahedral Mn forming a trimer connected further by carboxylate oxygens with two other square pyramidals Mn to form the pentamer.	[Mn$_5$O$_{20}$] pentanuclear	Antiferromagnetic χ_MT per Mn$_5$ unit at 300K = 16.83 emu mol^{-1} K θ = -138.9K Antiferromagnetic χ_MT per Mn$_5$ unit at 300K = 14.94emu mol^{-1} K θ = -210.1K
	Mn(3)	Distorted square-pyramid			
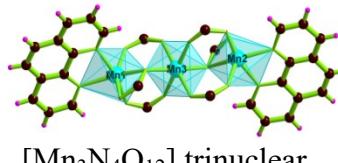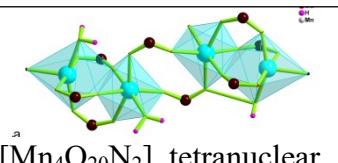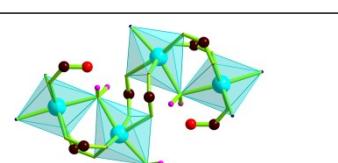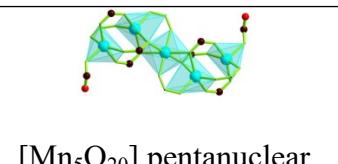
$[Mn_4(SBA)_4(DMA)_2]\cdot 3$ DMA[8]	Mn(1) Mn(2) Mn(3)	All adopt distorted octahedron	The Mn^{2+} ions are bonded through the carboxylate oxygens and the μ_2-O of the DMA molecules forming infinite Mn−O−Mn chains. The chains can be considered to be formed from trimeric $[Mn_3(CO_2)_6]$ units [Mn(1), Mn(2), and Mn(3)] connected by Mn(4) octahedra.	 $[Mn_3O_{12}]$ trinuclear	Antiferromagnetic $\chi_M T$ per Mn_4 unit at 300K = 17.4 emu mol^{-1} K θ = -26.7K
$[Mn_3(SBA)_3(DMA)_2(X)]\cdot DMA$. X=MeOH, EtOH, CH_3CN, ethylene glycol[8]	Mn(1) Mn(2) Mn(3)	Distorted octahedron Distorted square-pyramid	The Mn^{2+} ions form trimeric unit $[Mn_3(CO_2)_6]$.This trimer unit can be considered to be the secondary building unit for this structure. The connectivity between the trimer units and the SBA^{2-} anions initially forms a two-dimensional layer which is further bonded through SBA^{2-}anions leading to the formation of a three-dimensional structure	 $[Mn_3O_{12}]$ trinuclear	Antiferromagnetic $\chi_M T$ per Mn_3 unit at 300K = 14.1 emu mol^{-1} K θ = -41.2K
$[Mn(SBA)(dpap)]$.1.5H_2O[9]	Mn(1) Mn(2)	Distorted octahedron	Two polyhedra MnO_6 are bridged by the SBA^{2-}ligand and N-based donor to form the 3D structure	 $[MnO_6]$ discrete mononuclear	Not reported
$[H_3O][Mn_3(\mu_3\text{-}OH)(SBA)_3(H_2O)]\cdot(DMF)_5$[10]	Mn(1) Mn(2) Mn(3)	All adopt distorted octahedron	The Mn^{2+} ions are connected via the $\mu3$-OH as well as through the six carboxylate groups to form a triangular $[Mn_3(\mu_3\text{-}OH)(CO_2)_6]$ unit, which gives rise to a hexamer $[Mn_6(\mu_3\text{-}OH)_2(CO_2)_{12}]$ through symmetry translation. The Mn6 clusters are connected through pairs of SBA^{2-}anions forming a 2D layer	 $[Mn_6(OH)_2(CO_2)_{12}]$ hexanuclear	Antiferromagnetic $\chi_M T$ per Mn_3 unit at 300K = 18.6 emu mol^{-1} K θ = -107.1K
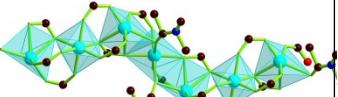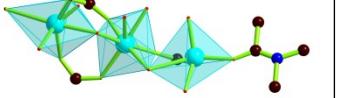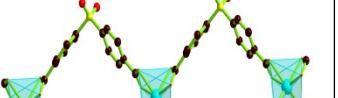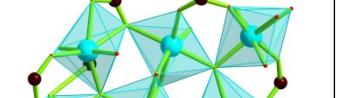
|					
[H$_3$O]$_2$[Mn$_7$(OH)$_4$(SBA)$_6$(H$_2$O)$_4$](H$_2$O)$_2$(DMF)$_8$[10]	Mn(1) Mn(2) Mn(3) Mn(4)	All adopt distorted octahedron	In solid a one-dimensional chain results from the connectivity between Mn7 clusters and SBA^{2-} anions. Two such chains are oriented in a direction that is mutually perpendicular to each other, forming the 2D layers. The layers are cross-linked by SBA^{2-} ions, giving rise to an anionic three-dimensional structure.	[Mn$_7$(μ$_3$-OH)$_4$(CO$_2$)$_{12}$] septanuclear	Antiferromagnetic χ_MT per Mn$_{3.5}$ unit at 300K =16.4 emu mol^{-1} K θ = -54.1K
[Mn$_3$(SBA)(bibp)(NO$_2$$^-$)$_2$(H$_2$O)$_2$]·2DMF[11]	Mn(1) Mn(2) Mn(3)	Distorted octahedron	Three neighboringMn (II) ions are connected by four carboxylate groups from four different SBA^{2-} ligands and two O atoms from two nitrite ions to form a linear trinuclear building block. The adjacent trinuclear building blocks are connected by ligands BIBP and SBA^{2-} to form an intriguing 3D network.	[Mn$_3$O$_{12}$N$_4$] trinuclear	Antiferromagnetic χ_MT per Mn$_3$ unit at 300K = 12.61cm^3 mol^{-1} K
(Me$_2$NH$_2$)[Mn$_4$(SBA)$_4$(HSBA)(H$_2$O)].3H$_2$O.2DMF[12]	Mn(1) Mn(2) Mn(3) Mn(4)	Distorted octahedron	In this solid Mn1O$_6$, Mn2O$_6$, Mn3O$_6$, and Mn4O$_6$ polyhedra are connected in other one by one via corner-sharing oxygen atoms to generate a Mn1-Mn2−Mn3−Mn4 unit. These infinite chains are then cross-linked by SBA^{2-} and HSBA$^-$ ligands to create a 3D framework	[Mn$_4$O$_{20}$] tetranuclear	Antiferromagnetic χ_MT per Mn$_4$ unit at 300K = 16.96 emu mol^{-1} K θ = -8.55K
[a]Abbreviations used: SBA, 4,4'-sulphonyldibenzoic acid (the ligand is also referred as sda and sdba in the literature); 2,2-bpy, 2,2-bipyridine; phen,1,10-phenanthroline; bpp/dpap, 1,3-bis(4-pyridyl) propane; btb, 1,4-bis(1,2,4-triazol-1-yl)butane; bim, 1,4-bis(imidazol-1-yl)butane; py, pyridine; 4-mepy, 4-picoline; bpp, 1,3-bi(pyridine-4-yl)propane; bibp, 4,4′-bisimidazolylbiphenyl					
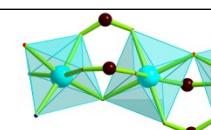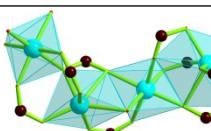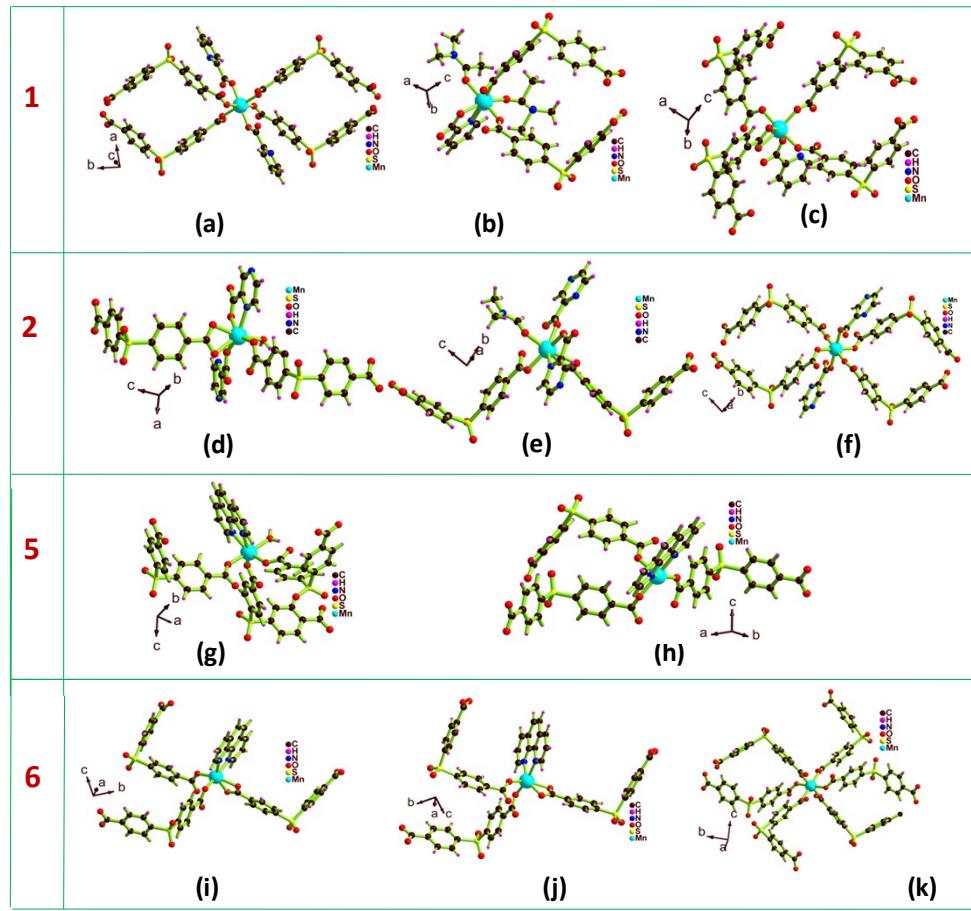
**Fig. S2** Coordination environment of Mn(II) in **1-6**

Fig. S3 Coordination modes of *SBA* with Mn(II) in **1-6**
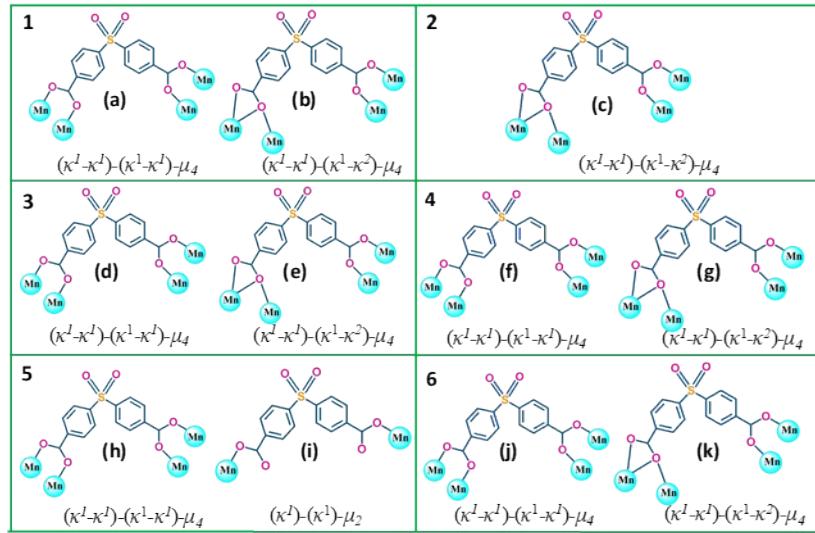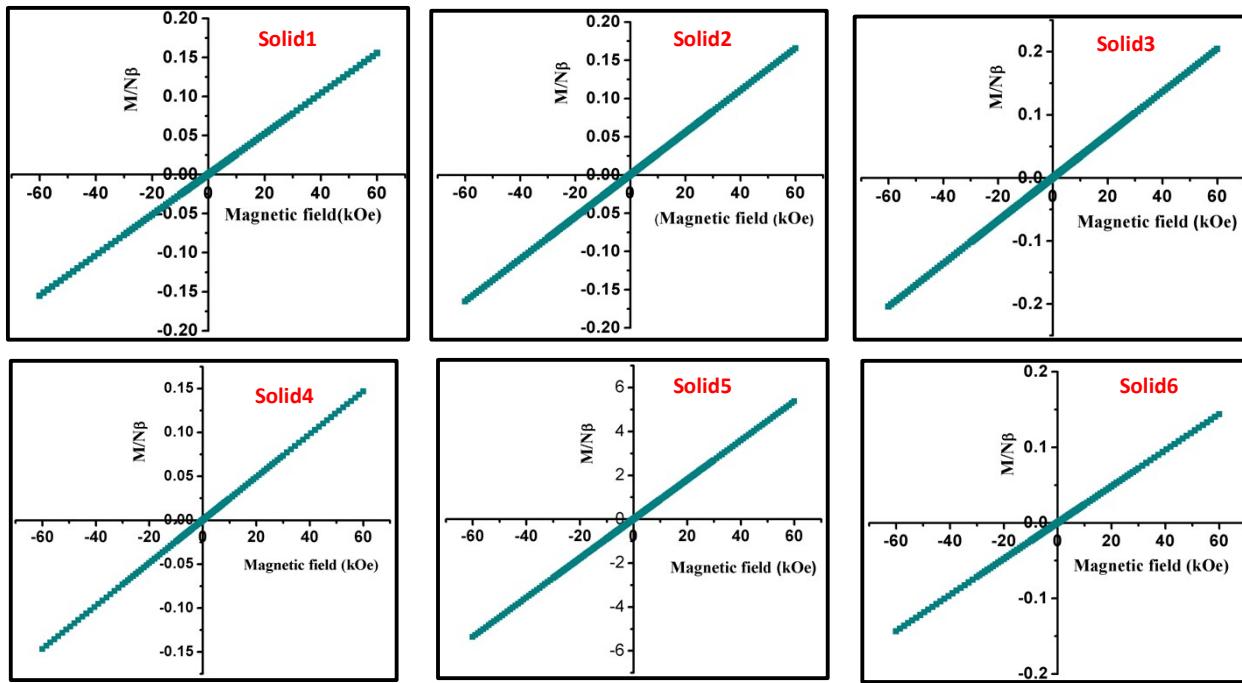
Fig S4. Field-dependent magnetization curve for **1-6** at 300K

Table S2 Selected bond lengths (Å) and angles (°) for **1-6**

1					
O9—Mn3	2.273(9)	O8^{iv}—Mn1—O10	88.91(25)	O1—Mn2—O2	86.55(26)
O11—Mn1	2.231(7)	O8—Mn1—O10	91.09(25)	O4—Mn2—O5	85.89(30)
O11—Mn3	2.320(9)	O10^{iv}—Mn1—O10	179.99(23)	O1—Mn2—O5	102.46(26)
O3—Mn3	2.203(8)	O8^{iv}—Mn1—O11	89.54(21)	O2—Mn2—O5	169.33(26)
O3—Mn2	2.221(9)	O8—Mn1—O11	90.46(21)	O4—Mn2—O3	105.92(27)
O10—Mn1	2.166(6)	O10^{iv}—Mn1—O11	91.58(21)	O1—Mn2—O3	157.30(25)
O4—Mn2	2.13(1)	O10—Mn1—O11	88.42(21)	O2—Mn2—O3	85.51(24)
O12—Mn3	2.148(9)	O8^{iv}—Mn1—O11^{iv}	90.46(21)	O5—Mn2—O3	88.09(24)
O6—Mn3	2.084(9)	O8—Mn1—O11^{iv}	89.54(21)	O4—Mn2—N1	174.20(29)
O2—Mn2	2.163(8)	O10^{iv}—Mn1—O11^{iv}	88.42(21)	O12—Mn3—O3	85.75(24)
O1—Mn2	2.139(8)	O10—Mn1—O11^{iv}	91.58(21)	O6—Mn3—O9	99.12(32)
O5—Mn2	2.201(9)	O11—Mn1—O11^{iv}	180.0(2)	O7—Mn3—O9	94.43(24)
O7—Mn3	2.129(9)	O4—Mn2—O1	94.96(33)	O12—Mn3—O9	89.64(26)
O8—Mn1	2.118(7)	O4—Mn2—O2	87.67(30)	O3—Mn3—O9	155.49(24)
Mn1—O8^{iv}	2.118(7)	O8^{iv}—Mn1—O8	180.00(23)	O6—Mn3—O11	155.78(27)
Mn1—O10^{iv}	2.166(6)	O8^{iv}—Mn1—O10^{iv}	91.09(25)	O7—Mn3—O3	91.67(22)
Mn1—O11^{iv}	2.231(7)	O8—Mn1—O10^{iv}	88.91(25)	O5—Mn2—N1	88.40(26)
Mn1—O11—Mn3	107.59(23)	O1—Mn2—N1	87.30(27)	O3—Mn2—N1	72.78(24)

Mn3—O3—Mn2	106.83(24)	O2—Mn2—N1	97.81(27)	O6—Mn3—O7	88.1(3)
O7—Mn3—O12	175.05(25)	O6—Mn3—O3	104.80(27)	O6—Mn3—O12	88.48(32)

Symmetry codes:(i) x, 1+y, z; (ii) 2-x, 1-y, -z; (iii) x, -1+y, z; (iv) 1-x, 1-y, 1-z

2					
Mn1—O8	2.277(3)	O8—Mn1—N3i	142.75(6)	Mn3—O2	2.135(7)
Mn1—O4i	2.272(4)	O4i—Mn1—O8	71.73(6)	Mn3—O5	2.142(5)
Mn1—O7	2.155(5)	O4i—Mn1—N3i	71.24(6)	Mn3—O3	2.153(5)
Mn1—O9	2.216(2)	O7—Mn1—O8	133.86(6)	Mn3—O6	2.094(7)
Mn1—N3i	2.324(6)	O7—Mn1—O4i	150.42(7)	O8ii—Mn2—N1ii	71.76(6)
Mn2—O8ii	2.256(3)	O7—Mn1—O9	85.97(7)	O4—Mn2—N1ii	143.35(6)
Mn2—O4	2.262(3)	O9—Mn1—O8	81.01(7)	O1—Mn2—O8ii	147.77(6)
Mn2—O1	2.190(5)	O9—Mn1—O4i	84.24(7)	O1—Mn2—O4	137.39(6)
Mn2—O20	2.211(3)	O8ii—Mn2—O4	72.31(6)	O1—Mn2—O20	85.36(7)

Symmetry codes: (i) -x, 2-y, 1-z; (ii) 1-x, 2-y, 1-z; (iii) 0.5-x, -0.5+y, 1.5-z; (iv) 0.5-x, 0.5+y, 1.5-z.

Solid 3					
O1—Mn1	2.123(4)	O16—Mn1i	2.189(4)	O5—Mn2—O2	175.08(12)
O2—Mn2	2.149(5)	O16—Mn2i	2.290(5)	O5—Mn2—O4	85.02(11)
O3—Mn1	2.155(3)	O15—Mn2i	2.292(5)	O5—Mn2—O16ii	88.65(10)
O4—Mn2	2.212(4)	O11—Mn3	2.177(4)	O5—Mn2—O15ii	90.42(11)
O5—Mn2	2.113(5)	O2—Mn2—O4	91.15(10)	O16ii—Mn2—C9ii	29.0(1)
O9—Mn3	2.123(4)	O2—Mn2—O16ii	94.94(10)	O16ii—Mn2—O15ii	57.23(10)
O12—Mn3	2.146(4)	O2—Mn2—O15ii	94.35(11)	O15ii—Mn2—C9ii	28.23(11)
O1—Mn1—O3	92.65(9)	O4—Mn2—C9ii	127.03(10)	O9—Mn3—O12	95.64(13)
O1—Mn1—O16ii	91.43(10)	O4—Mn2—O16ii	98.10(9)	O9—Mn3—O11	86.04(11)
O3—Mn1—O16ii	88.83(9)	O4—Mn2—O15ii	155.07(10)	O12—Mn3—O11	104.68(12)
O2—Mn2—C9ii	95.12(11)	O5—Mn2—C9ii	89.66(11)		

Symmetry codes:(i) x, -1+y, z; (ii) x, 1+y, z.

4					
Mn3—O3	2.155(4)	Mn2—O11i	2.238(7)	O1—Mn2—O00A	86.54(17)
Mn3—O10i	2.205(6)	Mn2—O1	2.108(8)	O1—Mn2—O11i	100.97(17)
Mn3—O18	2.129(7)	Mn1—O5	2.129(6)	O5—Mn1—O6	99.42(16)
Mn2—O10i	2.342(10)	Mn1—O6	2.183(8)	O2—Mn1—O5	97.60(16)
Mn2—O3	2.129(8)	Mn1—O2	2.118(7)	O18—Mn3—O10i	91.73(15)
O11i—Mn2—O10i	56.85(14)	O3—Mn3—O10i	93.12(13)	O5—Mn2—O10i	91.25(14)
O1—Mn2—O10i	157.56(15)	O18—Mn3—O3	89.48(14)	O6—Mn2—O11i	93.59(15)
Mn3ii—O10—Mn2ii	109.29(14)				

Symmetry codes:(i) x, -1+y, z; (ii) x, 1+y, z.

5					
O1—Mn1	2.186(8)	O10—Mn2	2.063(7)	O3—Mn1—O2	90.86(10)
O2—Mn1	2.173(5)	O8—Mn2	2.099(5)	O3—Mn1—O4	93.40(9)
O3—Mn1	2.122(7)	O2—Mn1—O1	88.8(1)	O4—Mn1—O1	89.04(9)
O7—Mn2	2.079(6)	O2—Mn1—O4	114.29(9)	O10—Mn2—O7	107.67(11)
O4—Mn1	2.18(1)	O3—Mn1—O1	177.45(10)		

Symmetry codes:
(i) x, -1+y, z; (ii) -1+x, y, z; (iii) 1+x, y, z; (iv) x, 1+y, z.

| 6					
Mn1—O6	2.154(2)	Mn2—O7	2.065(3)	O3—Mn1—O6	179.28(9)
Mn1—O3	2.143(2)	Mn3—O4	2.089(3)	O3—Mn1—O2	90.89(11)
Mn1—O2	2.191(3)	Mn3—O1	2.082(3)	O3—Mn1—O5	89.84(11)
Mn1—O5	2.203(3)	O6—Mn1—O2	89.65(11)	O2—Mn1—O5	178.59(10)
Mn2—O8	2.099(3)	O6—Mn1—O5	89.62(11)	O7—Mn2—O8	91.85(13)
(i) -x, 2-y, 1-z; (ii) 1-x, 2-y, 1-z; (iii) 0.5-x, -0.5+y, 1.5-z; (iv) 0.5-x, 0.5+y, 1.5-z.					

Solid 1

Solid 2

Solid 3
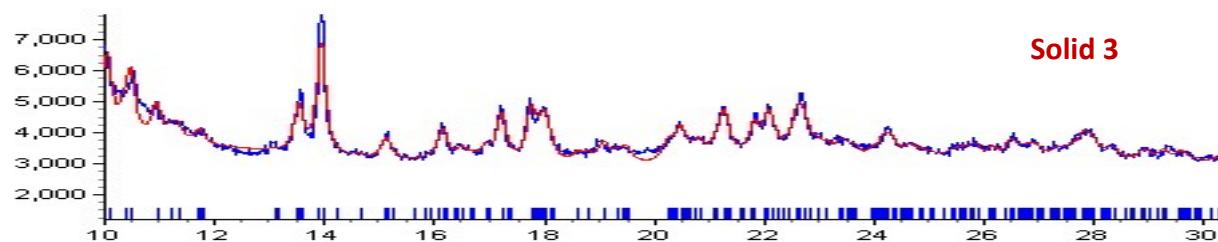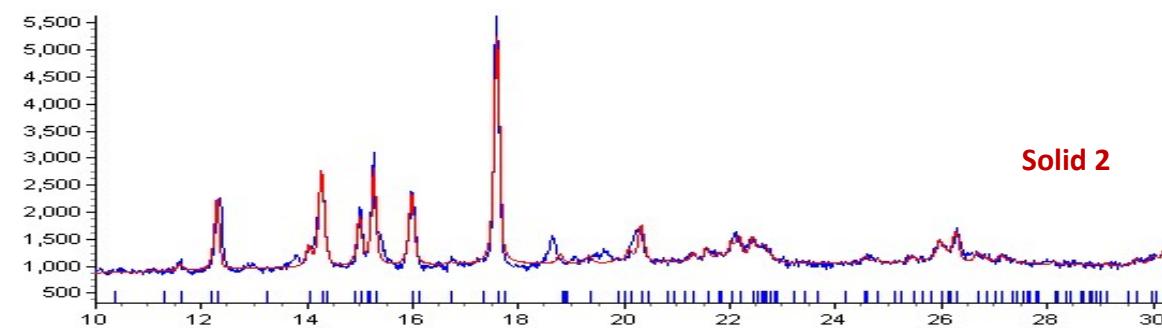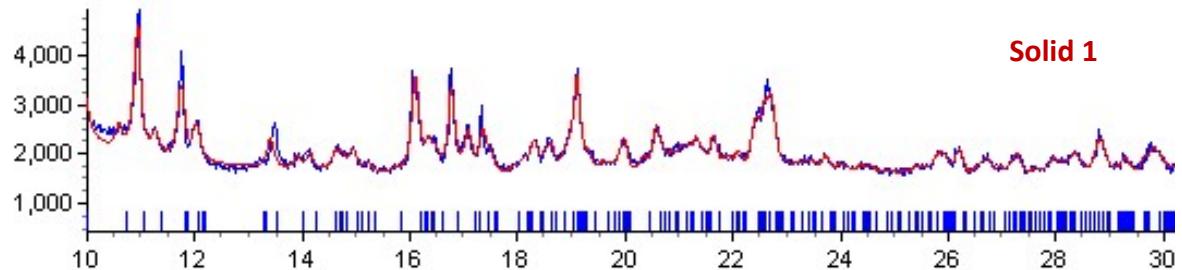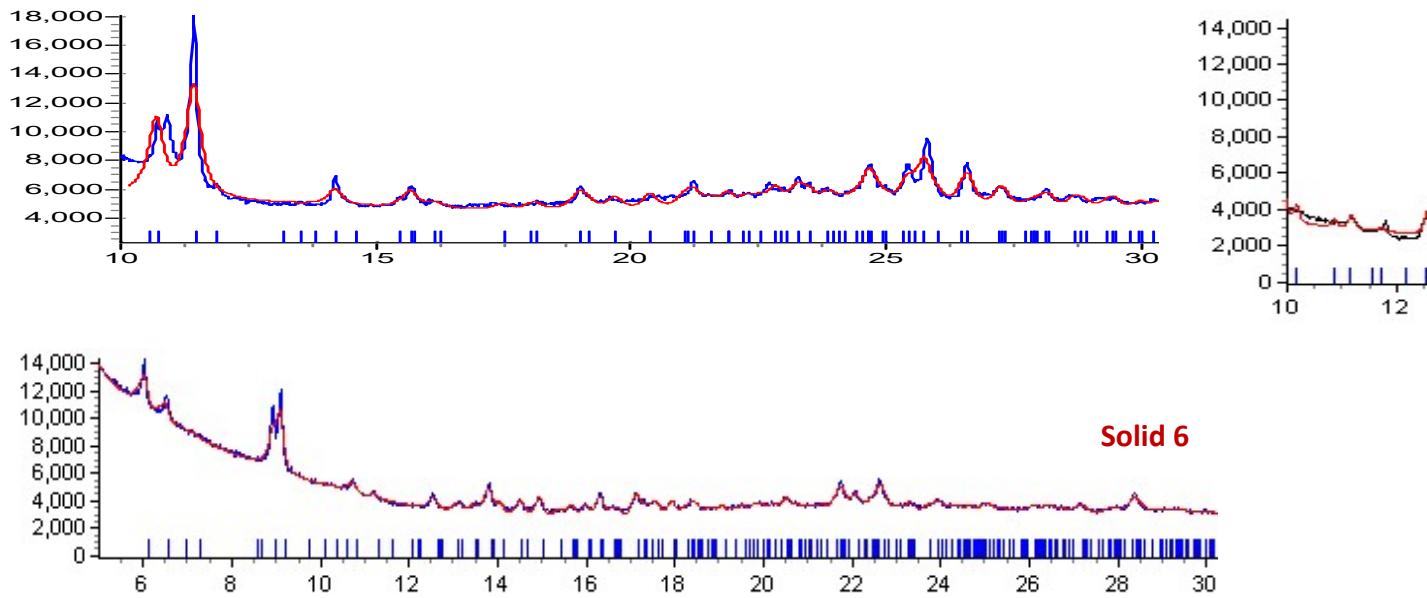
Fig S5: Rietveld refinement plots for **1-6**, indicating the homogeneity of the bulk samples. The plot shows the experimental powder XRD profile (blue line), the calculated (red line), and blue tick lines on the bottom show Bragg positions. Footnote: *Peak(s) marked with star correspond to an unidentified phase.
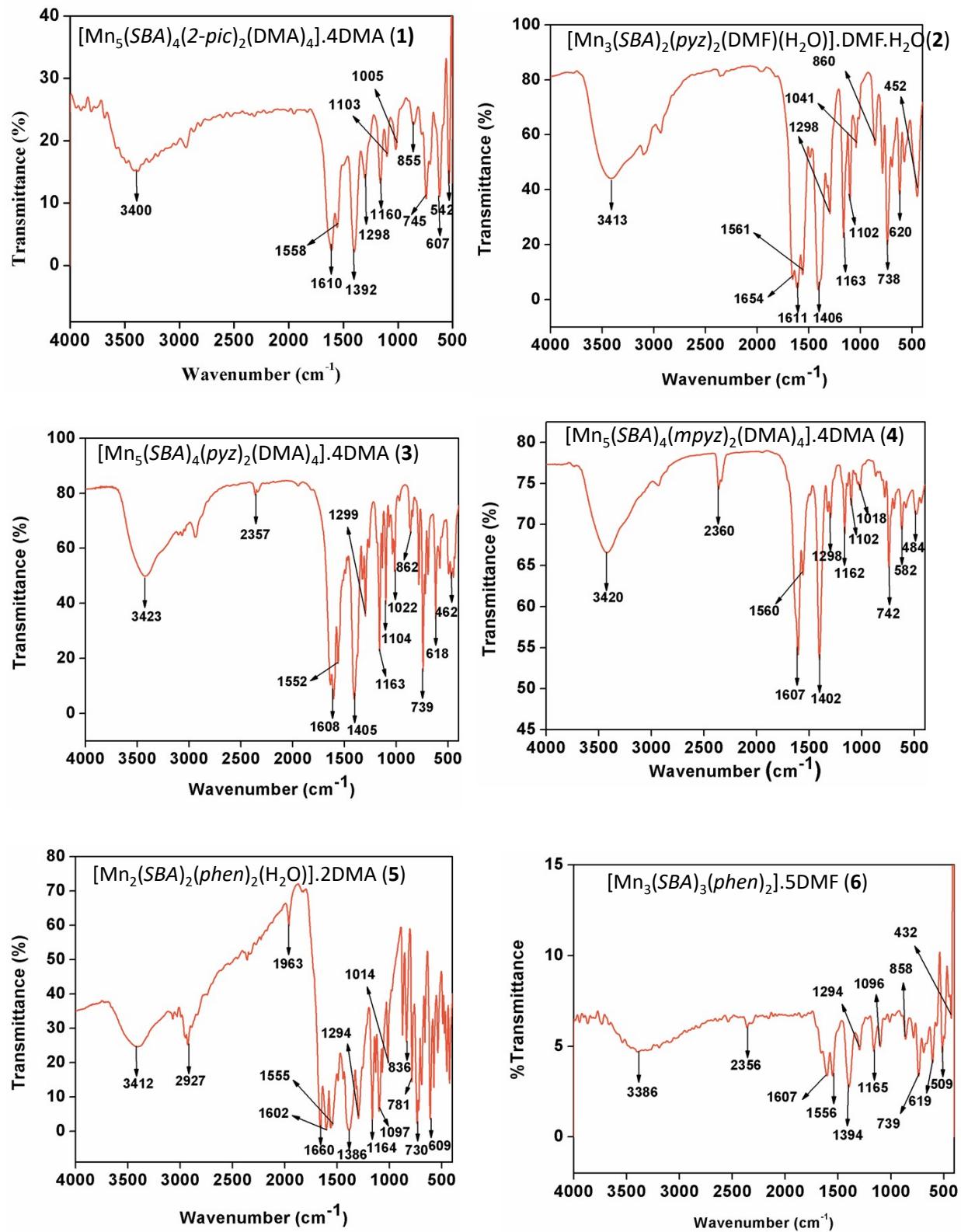
Fig S6: FT-IR spectra of **1-6**

Table S3: Selected vibrational frequencies for **1-6**

	1	2	3	4	5	6
	ν(cm^{-1})					
Mn-O stretch	542	452	462	484	490	509
C-S stretch	607	620	618	582	609	619
Mn-O-Mn Bending	745	738	739	742	730	739
S=O stretch	1005	1041	1022	1018	1014	1096
C-O stretch	1160	1163	1163	1162	1164	1165
C-N (solvent)	1298	1298	1299	1298	1294	1294
C=C (aromatic)	1558	1561	1552	1560	1555	1556
C=O (solvent)	1610	1611	1608	1607	1602	1607
-OH stretch	3400	3413	3423	3420	3412	3386

The vibrational spectra of **1-6** are quite comparable owing to the similarity in nature of bonds in these solids. Since all the six solids contain SBA in their structure, the peaks common among them are listed in Table S3. All solids displayed broad peak from 3400-3200 cm^{-1} corresponding to O-H stretching. Peaks from 1600-1620cm^{-1} depict the symmetric stretch of carboxylate while the peaks around 1560-1551cm^{-1} result from the asymmetric stretch of carbonyl group. Multiple sharp peaks ranging from 1600-1475cm^{-1} are from symmetric and antisymmetric stretch of C=C which is at lower end compared to isolated C=C depicting a partial single bond owing to resonance in the ring. Multiple Peaks from 1350cm^{-1} to 1000cm^{-1} are from the symmetric C-O and C-N bonds. Presence of peaks near 790cm^{-1} and 840cm^{-1} indicate the para-substitution of phenyl rings. The stretching peaks near 745-710cm^{-1} depict the presence of Mn-O-Mn bond. The stretching peaks near 800-600cm^{-1} and around 1010 cm^{-1} depicts the presence of C-S and S=O bonds, respectively. Mn-O symmetric stretch appears near 540-450cm^{-1}.

References:

1 C. R. Groom, I. J. Bruno, M. P. Lightfoot and S. C. Ward, *Acta Crystallogr. Sect. B Struct. Sci. Cryst. Eng. Mater.*, 2016, **72**, 171–179.

2 S.-W. Yan, G.-J. Zhang, H.-Y. Chen, S.-C. Chang and F.-T. Zhang, *Acta Crystallogr. Sect. E Struct. Rep. Online*, 2011, **67**, m712–m712.

3 H. Chen, D. Xiao, J. He, Z. Li, G. Zhang, D. Sun, R. Yuan, E. Wang and Q.-L. Luo, *CrystEngComm*, 2011, **13**, 4988.

4 D. Xiao, R. Yuan, Y. Chai and E. Wang, *Eur. J. Inorg. Chem.*, 2008, **2008**, 2610–2615.

5 C.-Y. Wu, D. S. Raja, C.-C. Yang, C.-T. Yeh, Y.-R. Chen, C.-Y. Li, B.-T. Ko and C.-H. Lin, *CrystEngComm*, 2014, **16**, 9308–9319.

6 N. Li, L. Chen, F. Lian, F. Jiang and M. Hong, *Inorganica Chim. Acta*, 2010, **363**, 3291–3301.

7 S. Bhattacharya, K. V. Ramanujachary, S. E. Lofland, T. Magdaleno and S. Natarajan, *CrystEngComm*, 2012, **14**, 4323.

8 S. Bhattacharya, A. J. Bhattacharyya and S. Natarajan, *Inorg. Chem.*, 2015, **54**, 1254–1271.

9 C.-J. Wang, Y.-Y. Wang, J.-Q. Liu, H. Wang, Q.-Z. Shi and S.-M. Peng, *Inorganica Chim. Acta*, 2009, **362**, 543–550.

10 S. Bhattacharya, M. Gnanavel, A. J. Bhattacharyya and S. Natarajan, *Cryst. Growth Des.*, 2014, **14**, 310–325.

11 C.-L. Zhang, L. Qin and H.-G. Zheng, *Inorg. Chem. Commun.*, 2013, **34**, 34–36.

12 C.-B. Tian, C. He, Y.-H. Han, Q. Wei, Q.-P. Li, P. Lin and S.-W. Du, *Inorg. Chem.*, 2015, **54**, 2560–2571.